Carbohydrate Polymers 98 (2013) 896–904

Contents lists available at SciVerse ScienceDirect

Carbohydrate Polymers

journal homepage: www.elsevier.com/locate/carbpol

Novel phosphorus-containing cyclodextrin polymers and their affinity for calcium cations and hydroxyapatite

Véronique Wintgens, Florent Dalmas, Bernard Sébille, Catherine Amiel*

Systèmes Polymères Complexes, ICMPE, 2-8 Rue Henry Dunant, 94320 Thiais, France

ARTICLE INFO

Article history:
Received 29 May 2013
Received in revised form 27 June 2013
Accepted 28 June 2013
Available online 7 July 2013

Keywords:
β-Cyclodextrin
Phosphated cyclodextrin polymer
Hydroxyapatite
Nanoparticles
Calcium binding capacity

ABSTRACT

Novel phosphorous-containing β-cyclodextrin (βCD) polymers (CDP) were synthesized easily under "green chemistry" conditions. A simple polycondensation between the hydroxyl groups of βCD and non-toxic sodium trimetaphosphate (STMP) under basic conditions led to soluble, non-reticulated CDPs with molecular weights (M_w) higher than 10^4 g mol^{-1}, the actual value depending on the NaOH:βCD and STMP:βCD weight ratios. The presence of both βCD and phosphate groups in the polymer allows for strong interactions with amphiphilic probes, such as 1-adamantyl acetic acid, or with divalent cations, such as Ca^{2+}, whose strengths were characterized by isothermal titration microcalorimetry. The obtained phosphated compounds also display high affinity towards hydroxyapatite (HA), leading to HA nanoparticles that could easily be recovered by CDPs, as demonstrated by transmission electron microscopy and quantitative determination of the total amount of phosphated molecules fixed on HA.

1. Introduction

Phosphorus-containing polymers are highly attractive materials due to the large range of technological applications that are directly related to the presence of phosphorus-derived functional groups in the polymer. They have been used for instance as flame-retardants (Ai, Xu, Liu, Chen, & Zhang, 2009; Xia et al., 2006), ion-exchange resins (Grachek, Shunkevich, & Martsynkevich, 2011), dental adhesives (Akgun, Savci, & Avci, 2012), or adhesion promoters on metal surfaces (Lakshmi, Ashwaq, & Reddy, 2011). Recently, their biodegradability, hemocompatibility and protein adsorption resistance have led to numerous developments in the biomedical field (Chaubal, Gupta, Lopina, & Bruley, 2003; Huang & Zhuo, 2008). A recent review describes the use of phosphorus-containing polymers in various applications such as in dentistry, regenerative medicine and drug delivery (Monge, Canniccioni, Graillot, & Robin, 2011). Incorporation of phosphonic groups into monomers was proposed, for example, as a way to increase biocompatibility and adhesion to the tooth by chelation with calcium ions on the tooth surface (Mou, Singh, & Nicholson, 2000). Functionalization of polymer scaffolds with phosphate groups has also been used to initiate in vitro calcium phosphate mineralization (Suzuki, Whittaker, Grøndahl, Monteiro, & Wentrup-Byrne, 2006). In another example, immobilization of cysteamine, a chemical radioprotector, on poly(oxyalkylene phosphates) used as a drug carrier was shown to induce a significant toxicity decrease (Georgieva et al., 2002). Finally, the high affinity of phosphates and phosphonates towards transition metals has led some authors to use a phosphated carboxymethyl cellulose to functionalize titanium oxide surfaces (Pasqui, Rossi, Di Cintio, & Barbucci, 2007). The obtained TiO_2 surfaces featured better biocompatibility and bonelike cells growth performances, potentially improving osseointegration.

Another structural residue that has shown great promise in biomaterials as a biocompatible, high-affinity ligand is the cyclodextrin ring. Cyclodextrins (CDs) are cyclic oligosaccharides, made of 6, 7 or 8 α-D-glucopyranose units, forming toroidal-shaped molecules with an hydrophilic outer surface and an hydrophobic cavity suitable for inclusion complexation with various lipophilic compounds (Li & Purdy, 1992). Due to their oligosaccharide structure, they contain several hydroxyl groups that can possibly be used for further functionalization or for covalent coupling to other structures (Khan, Forgo, Stine, & D'Souza, 1998). They are widely used in science and industry (Szejtli, 2004; Uekama, 2004; Loftsson & Duchêne, 2007; Bilensoy, 2011). In biomaterials, they have particularly been used as delivery agents. For example, porous hydroxyapatite (HA) pellets have been functionalized with cyclodextrin polymers capable of loading and progressively releasing lipophilic antibiotics (Leprêtre et al., 2009). This approach helped in overcoming the infection induced by HA calcium phosphate bioceramics used in bone regeneration applications, as well as in dental and orthopaedic surgery to fill bone defects and coat metallic implant surfaces.

Systems exhibiting a combination of phosphorus-containing functional groups and cyclodextrin rings have been described

* Corresponding author. Tel.: +33 1 49781219; fax: +33 1 49781208.
E-mail address: amiel@icmpe.cnrs.fr (C. Amiel).

0144-8617/$ – see front matter © 2013 Elsevier Ltd. All rights reserved.
http://dx.doi.org/10.1016/j.carbpol.2013.06.073

as well. For instance, an alendronate-β-cyclodextrin conjugate designed for local delivery of therapeutic agents to bones and teeth used the two residues to load and release a drug via the βCD cavity and to bind to HA via a bisphosphonate group (Liu, Lee, Reinhardt, Marky, & Wang, 2007). This CD derivative also demonstrated promising in vivo bone anabolic effects (Liu et al., 2008). In another example, a βCD was grafted onto a hydroapatite/beta-tricalcium phosphate surface that had previously been modified via a two-step reaction (Jacobsen, Nielsen, Juhl, Theilgaard, & Larsen, 2012). The authors used a lipophilic fluorescent probe to show that cyclodextrins can load and release specific lipophilic molecules.

The project whose results are reported in the present contribution aimed at synthesizing novel, structurally simple phosphorus-containing CD polymers using "green chemistry", and at evaluating their performances in drug complexation and HA interactions. Indeed, polymers that combine cyclodextrin and phosphorus functionalities would be perfectly suited for biomedical applications that jointly require calcium affinity and transport/delivery of lipophilic bioactive molecules. As a novel route to these phosphated CD polymers (CDP), sodium trimetaphosphate (STMP), a non-toxic cyclic triphosphate, is considered in this reported work as a possible "green" polymer-modifying agent.

STMP is known to react with hydroxyl groups to form phosphates. It is largely used as a cross-linking agent for hydroxylated polymers, the resulting cross-linked hydrogels having found numerous applications. For example, Letourneur et al. developed hydrogels made of dextran and pullulan, which have recently been proposed as biomaterials for tissue engineering applications (Abed et al., 2011; Autissier, Letourneur, & Le Visage, 2007; Autissier, Visage, Pouzet, Chaubet, & Letourneur, 2010). In other applications of such hydrogels, bare metal stents have been covered by a STMP cross-linked, cationized pullulan hydrogel capable of loading and delivering siRNA (San Juan et al., 2009), or vascular grafts have been prepared with cross-linked poly(vinyl alcohol) (Chaouat et al., 2008). In addition, the rheological properties of SMTP cross-linked xanthan (Bejenariu, Popa, Dulong, Picton, & Le Cerf, 2009) and pullulan (Lack et al., 2004) hydrogels have been investigated, together with their swelling, loading and release behaviour (Bejenariu et al., 2009). Several studies have reported the properties of SMTP cross-linked starches (Khondkar, Tester, Hudson, Karkalas, & Morrow, 2007; Le Bail, Morin, & Marchessault, 1999; Sang, Prakash, & Seib, 2007; Sang, Seib, Herrera, Prakash, & Shi, 2010; Woo & Seib, 1997) that are mainly used as food thickeners, as STMP is one of the few cross-linkers authorized in foodstuff. Additionally, STMP has also been used to prepare microparticles by emulsion cross-linking from starch (Li et al., 2009) or pullulan (Mocanu, Mihai, Picton, LeCerf, & Muller, 2002). In summary, STMP is currently and extensively used to crosslink pre-existing polymers (such as polysaccharides), but – to the best of our knowledge – no references in the literature are available on a polymer that would have been synthesized by STMP polycondensation with a monomer bearing more than two hydroxyl groups. Reaction of STMP with βCD has been reported though, resulting in the formation of cyclodextrin monophosphates (Tarelli, Lemercinier, & Wheeler, 1997) and triphosphates (Inoue, Nakayama, & Tsuhako, 2000; Inoue, Tone, Nakayama, & Tsuhako, 2003).

The present contribution aims at investigating whether soluble, non-reticulated phosphorus-containing polymers (CDP) can be synthesized in a very straightforward manner, by just mixing a CD and SMTP under conditions that would favour polycondensation. In this work, such experimental conditions have been optimized, and polymers with molecular weight (M_w) higher than 10^4 g mol^{-1} have been obtained. The synthetic conditions are described in the first part of this paper, the polymers being characterized by elementary analysis, inductively coupled plasma atomic emission spectroscopy (ICP-AES), size exclusion chromatography (SEC) and ^{31}P nuclear magnetic resonance (NMR). In the second part, we demonstrate by isothermal titration microcalorimetry (ITC) that the obtained CDP are still active in forming inclusion complexes, and that the presence of phosphated groups leads to strong interactions with a divalent cation, Ca^{2+}. Finally, in the last section, we highlight interactions between these novel phosphorus-containing cyclodextrin polymers and HA.

2. Experimental

2.1. Materials

βCD was a gift from Roquette (France), and was used as received for the polymer synthesis but recrystallized in water for the ITC experiments. Sodium trimetaphosphate (STMP), sodium hydroxide, calcium chloride and hydroxyapatite ($Ca_5(OH)(PO_4)_3$, particles size <200 nm, surface area >9.4 m^2 g^{-1}, ref 677418) were purchased from Sigma–Aldrich (France) and used as received. Water was of deionized quality for the synthesis and of ultrapure quality for the other experiments.

2.2. Synthesis

Typically, 10 g of βCD were dissolved in 20 mL of a NaOH solution (with NaOH:βCD weight ratios of 8, 20 and 40 wt.%, corresponding to [NaOH] of 1.0, 2.5 and 5.0 mol L^{-1}, respectively), under mechanical stirring (300 rpm) at 30 °C. After 210 min, the temperature was raised to 50 °C, and the desired amount of STMP was added to the solution under vigorous stirring (600 rpm). After 90 min, 100 mL of water were added, and the pH was adjusted to 6.5 by HCl addition. The solution was dialyzed against water (molecular weight cut-off of 3500) and freeze-dried. Experimental conditions are provided in Table 1, along with identifying codes for the βCD polymers (CDP-*x*-*y*), *x* and *y* referring to the NaOH:βCD and STMP:βCD weight ratios, respectively.

2.3. Samples preparation

All solutions were prepared in ultrapure water, and those containing CDP left to equilibrate at least 1 day before the experiments.

To visually follow the interactions between CDP and $CaCl_2$, 0.6 mL of a $CaCl_2$ solution was set in a small flask with magnetic stirring at 300 rpm, and 0.6 mL of a CDP solution was rapidly added. Concentrations of both solutions were selected in order for the Ca^{2+}:P molar ratios and CDP concentrations to be varied ($1 < Ca^{2+}:P < 4.5$ and $5\ g\ L^{-1} < CDP < 50\ g\ L^{-1}$).

The minimum time that HA and CDP must be in contact to provide the highest coverage of the HA nanoparticles was estimated as follows: 25 mg of HA were weighed in 5 flasks, and 10 mL of a CDP-20-150a solution (0.2 g L^{-1}) were added. The flasks were immersed in an ultrasonic bath, and one of the flasks was removed after 15, 30, 60, 120 and 240 min, respectively. After centrifugation, the total carbon (TC) concentration of supernatants was determined. The TC value was constant for samples that had been kept at least 60 min in the ultrasonic bath.

The amount of CDP fixed on the HA nanoparticles was obtained as follows: various amounts of HA (0, 10, 20, 30, 40 and 50 mg) were weighed in 6 flasks, and 10 mL of a CDP-20-150a or a CDP-8-30 solution at 0.2 g L^{-1} were added. After at least 60 min in an ultrasonic bath and centrifugation, the TC concentration of supernatants was determined.

Table 1
Experimental conditions for the synthesis of CDPs, along with the isolated material, IM (% relative to the βCD initial weight), molecular weights, and carbon, phosphorus and βCD contents of the recovered polymers.

Polymer	NaOH:βCD (wt.%)	STMP:βCD (wt.%)	t (min)	T (°C)	IM (%)	M_n (g mol^{-1})	M_w (g mol^{-1})	PDI	C (wt.%)	βCD (wt.%)	P (wt.%)
CDP-8-10	8	10	90	50	9.6	2.80×10^3	3.1×10^3	1.1	35.5	79.9	2.3
CDP-20-10	20				13.6	1.70×10^3	2.1×10^3	1.2	35.7	80.4	1.8
CDP-8-30	8	30	90	50	21.9	3.50×10^3	6.2×10^3	1.7	33.8	76.1	3.3
CDP-8-60	8	60	90	50	10.0	3.45×10^3	4.7×10^3	1.3	29.7	66.8	6.1
CDP-20-60a	20				10.7	4.97×10^3	8.64×10^3	1.7	31.2	70.3	3.8
CDP-20-60b					16.6	13.0×10^3	33.4×10^3	2.5	30.8	69.4	4.2
CDP-20-60c					17.0	10.0×10^3	25.9×10^3	2.6	31.8	71.6	4.8
CDP-40-60a	40				2.8[a]	2.5×10^3	3.4×10^3	1.3	30.8	69.3	4.4
CDP-40-60b					15.0	2.8×10^3	3.4×10^3	1.2	29.6	66.7	4.9
CDP-40-60c					4.5[a]	2.7×10^3	3.6×10^3	1.4	30.5	68.7	5.4
CDP-8-100	8	100	90	50	13.4	3.7×10^3	5.3×10^3	1.4	28.2	63.5	6.3
CDP-20-100	20				8.1	9.4×10^3	29.7×10^3	3.2	29.7	66.8	5.9
CDP-8-150	8	150	90	50	17.9	4.4×10^3	6.6×10^3	1.5	28.8	64.9	6.0
CDP-20-150a	20				23.8	16.1×10^3	59.2×10^3	3.0	28.5	64.2	5.6
CDP-20-150b					24.0	12.9×10^3	41.8×10^3	3.2	27.9	62.8	5.6
CDP-20-150c				80	16.6	6.3×10^3	14.8×10^3	2.3	30.6	68.9	5.5
CDP-20-150d			180	50	14.4	12.2×10^3	36.2×10^3	3.0	30.3	68.2	6.6
CDP-20-150e					14.5	15.9×10^3	54.0×10^3	3.4	29.1	65.5	5.4
CDP-20-150f			990		19.1	10.1×10^3	32.4×10^3	3.3	29.2	67.8	5.7
CDP-40-150	40		90		13.6	5.4×10^3	12.3×10^3	2.3	28.1	63.3	6.2
CDP-8-200	8	200	90	50	9.5	4.1×10^3	5.6×10^3	1.3	28.2	63.5	6.3
CDP-20-200	20				11.6	13.2×10^3	49.6×10^3	3.7	28.6	64.4	6.0

[a] Perforated dialysis bag.

2.4. Instrumentation

Elemental analysis (C wt.%) were performed at the Institut de Chimie des Substances Naturelles (Gif sur Yvette, France). The Inductively Coupled Plasma Optical Emission Spectrometry (ICP-OES) analysis (P wt.%) were carried out at ICMPE (Thiais, France) with a ICP-OES spectrometer (Simultaneous Varian Vista Axial) using a 0.1 g L^{-1} deionized water solution of the polymers.

Total carbon analyses (TC) were obtained with a TOC-L CSN from Shimadzu. A potassium hydrogen phthalate solution in ultrapure water (0.53125 g L^{-1} corresponding to 250 mg C L^{-1}) was used to establish a calibration curve in the 5–250 mg C L^{-1} range.

Size exclusion chromatography coupled to multi-angle laser light scattering (SEC-MALLS) was performed in deionized water with 0.1 mol L^{-1} $LiNO_3$ (0.05% NaN_3) (columns TSK-gel type SW 4000–3000 and detection by a Wyatt Dawn 8+ light scattering detector and a Wyatt Optilab Rex refractive index detector).

^{1}H, ^{13}C and ^{31}P NMR spectra were recorded in deuterated water with a Brucker 400 MHz spectrometer.

Isothermal titration microcalorimetry (ITC) was carried out using a MicroCal VP-ITC microcalorimeter as previously reported for titrations by CDs (Layre, Wintgens, Gosselet, Dalmas, & Amiel, 2009). The experimental data were fitted with a theoretical titration curve corresponding to a 1:1 complex formation, using the software developed by MicroCal. The enthalpy change, ΔH, the association constant, K, and the overall stoichiometry, n, were used as adjustable parameters.

Transmission electron microscopy (TEM) observations were conducted on a FEI Tecnai F20 ST microscope (field-emission gun operated at 3.8 kV extraction voltage) operating at an acceleration voltage of 200 kV. The use of a minimal dose system was necessitated by the electron radiation sensitivity of the polymer corona. All the observations were performed at −170 °C, except for HA that was observed at room temperature. The samples were prepared as follow: a 15 μL drop of the HA suspension (0.1 g L^{-1}) was deposited on a carbon coated 400 mesh copper grid that had previously been treated by air plasma for 120 s. The excess of solution was then blotted with filter paper after 60 s.

3. Results and discussion

3.1. Synthesis

The mechanism of saccharide cross-linking by STMP has already been established from ^{31}P NMR studies on a model compound, α-D-glucopyranoside (Lack, Dulong, Picton, Cerf, & Condamine, 2007), and transposed to polysaccharides (pullulan (Lack et al., 2007), xanthan (Bejenariu et al., 2009) and starch (Sang et al., 2007)). Fig. 1 summarizes the main proposed steps: (a) transformation of the hydroxyl groups into alcoholates by NaOH, (b) opening of STMP either by NaOH, leading to sodium tripolyphosphate (STPP), or by the formed alcoholate, giving grafted tripolyphosphate (TPPg),

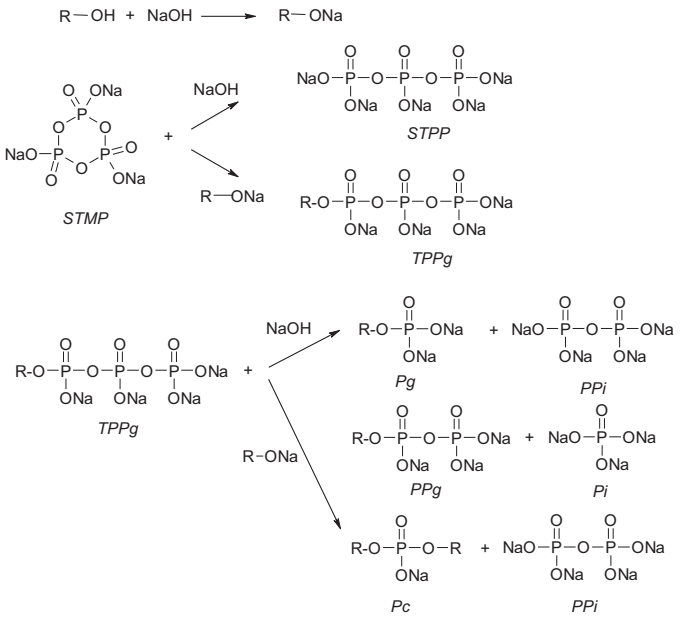

Fig. 1. Mechanism proposed in the literature (see text) for the cross-linking of polysaccharides by STMP.

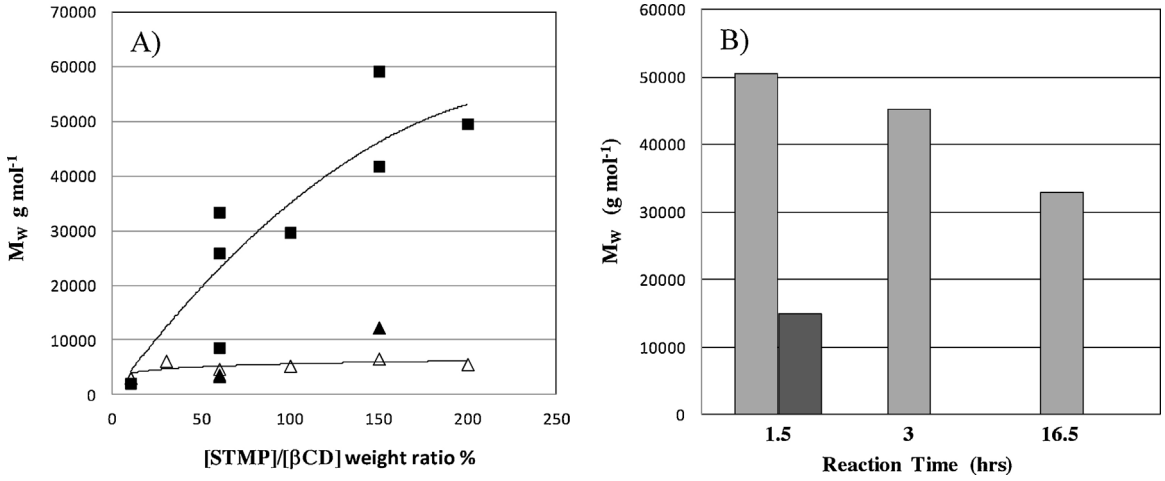

Fig. 2. M_w of CDPs as a function of (A) STMP:βCD weight ratio at NaOH:βCD weight ratios of 8% (△), 20% (■) or 40% (▲), and (B) reaction time at 50 °C (■) and 80 °C (■) with NaOH:βCD and STMP:βCD weight ratios of 20% and 150%, respectively.

an intermediate in the cross-linking reaction. In a third and final step (c), TPPg reacts either with the alcoholate giving phosphate diester (Pc), or with NaOH mainly leading to grafted monophosphate (Pg), the by-products being inorganic pyrophosphate (PPi). Grafted pyrophosphate (PPg) along with inorganic phosphate (Pi) can also be produced, generally formed in negligible amount (Lack et al., 2007; Sang et al., 2007). Only molecules with one phosphorus linking two sugars (Pc) have been identified, the experimental conditions determining the ratio observed between Pc and Pg (Lack et al., 2007). For example, Pc is not obtained at high NaOH concentrations as degradation reactions prevail, yielding mainly Pg, PPi and STPP.

The action of STMP on α- and βCD also depends on the experimental conditions. In the solid phase at 90 °C, only CD monophosphates have been obtained (Tarelli et al., 1997), while in diluted CD solutions (7.5 wt.%), reaction of STMP at pH 12 led to CD tripolyphosphates (Inoue et al., 2000, 2003). In analogy with the works performed on α-D-glucopyranoside (Lack et al., 2007) and polysaccharides (Lack et al., 2007; Sang et al., 2007; Bejenariu et al., 2009), some experimental conditions (involving reagents concentrations and pH) should nevertheless be available to ensure the formation of phosphate linking units between βCDs, and obtain phosphated βCD polymers via a simple mixing of βCD with STMP in alkaline medium, the obtained polymer having high enough molecular weight (i.e. higher than 10^4 g mol^{-1}) to display a significant amount of βCD units.

As a result, we explored several experimental conditions, varying NaOH:βCD and STMP:βCD weight ratios, reaction time and temperature as experimental variables (see Table 1). No gelation could be observed whatever the experimental conditions, suggesting that STMP is not a strong coupling agent for CDs in contrast to other agents such as epichlorohydrin (Renard, Deratani, Volet, & Sébille, 1997) or other bifunctional agents where gelation is most often observed (Ansari, Vavia, Trotta, & Cavalli, 2011; Cesteros, Ramírez, Peciña, & Katime, 2007; García-Zubiria, González-Gaitanoa, & Isasi, 2007; Pariot, Edwards-Lévy, Andry, & Lévy, 2000). Highly concentrated βCD (50 wt.%) solutions were used in order to promote Pc formation, along with strong alkaline conditions, the NaOH:βCD weight ratios being varied from 8 to 40 wt.%. STMP was added at once in the βCD alkaline solution, with STMP:βCD weight ratios included between 10 and 200 wt.%. A first series of experiments were conducted at 50 °C with a reaction time of 1h30. After extensive dialysis against water (using a membrane cut-off of 3500), several grams of a white solid were generally obtained (see Table 1), with isolated material percentage (relative to the βCD initial weight) included between 10 and 24%.

The presence of carbon and phosphorus in the obtained polymers was evidenced by elemental and ICP-OEP analysis, respectively. The obtained results are reported in Table 1. The βCD content in the CDPs (wt.%), as calculated from carbon wt.%, g L^{-1} ranges from 63% to 80%, the highest values being obtained for synthesis performed with the lowest STMP:βCD weight ratios. In addition, the phosphorus weight percentage increases from 2 to 6 when the STMP:βCD weight ratio increases from 10 to 60%. For higher STMP:βCD weight ratios, the phosphorus weight percentage is practically constant, at about 6 wt.%. Using the above values, one can calculate that the number of phosphorus atoms per βCD unit increases from ~1 to ~4 in the polymer. It should be noted however that, among the phosphorus atoms, only some of them are included in the monophosphate units connecting the βCD repeat units. Additionally, the above numbers are low compared to numbers obtained experimentally when epichlorohydrin (EP) is reacted with βCD under similar conditions. In this case, numbers as high as 16 have been reported under specific conditions, inducing gelation (Renard et al., 1997). Considering that, the probability that one βCD is bond to more than two other βCD is much lower in our case than with epichlorohydrin.

CDP absolute weight-average molecular weights M_w were determined by SEC-MALLS, the results being reported in Table 1 (examples of chromatograms are also provided in Figure S1, Supporting Information). Fig. 2A summarizes how M_w is affected by the STMP:βCD weight ratio for several NaOH:βCD ratios, and indicates that M_w strongly depends on both. For the lowest and highest NaOH:βCD weight ratios, M_w values range below 10^4 g mol^{-1}, varying the STMP:βCD weight ratio having almost no effect on M_w. Moreover, for a NaOH:βCD weight ratio of 20%, M_w increases with the STMP:βCD weight ratio, and reaches values as high as 5.9×10^4 g mol^{-1}. The polydispersity indices (PDI = M_w/M_n) for the polymers with $M_w > 10^4$ g mol^{-1} are large (~3), as expected for such a polycondensation reaction.

We also checked the effect of the reaction time and temperature for experiments performed with NaOH:βCD and STMP:βCD weight ratios of 20% and 150%, respectively. As shown in Fig. 2B, increasing the reaction time slightly decreases M_w. Otherwise, increasing the temperature to 80 °C leads to much lower M_w. This fall can be attributed either to a partial hydrolysis of the phosphate diester functional groups (Pc) that would result from an increase in reaction time or temperature or to a more significant opening of STMP by NaOH, leading to inactive STPP by-products.

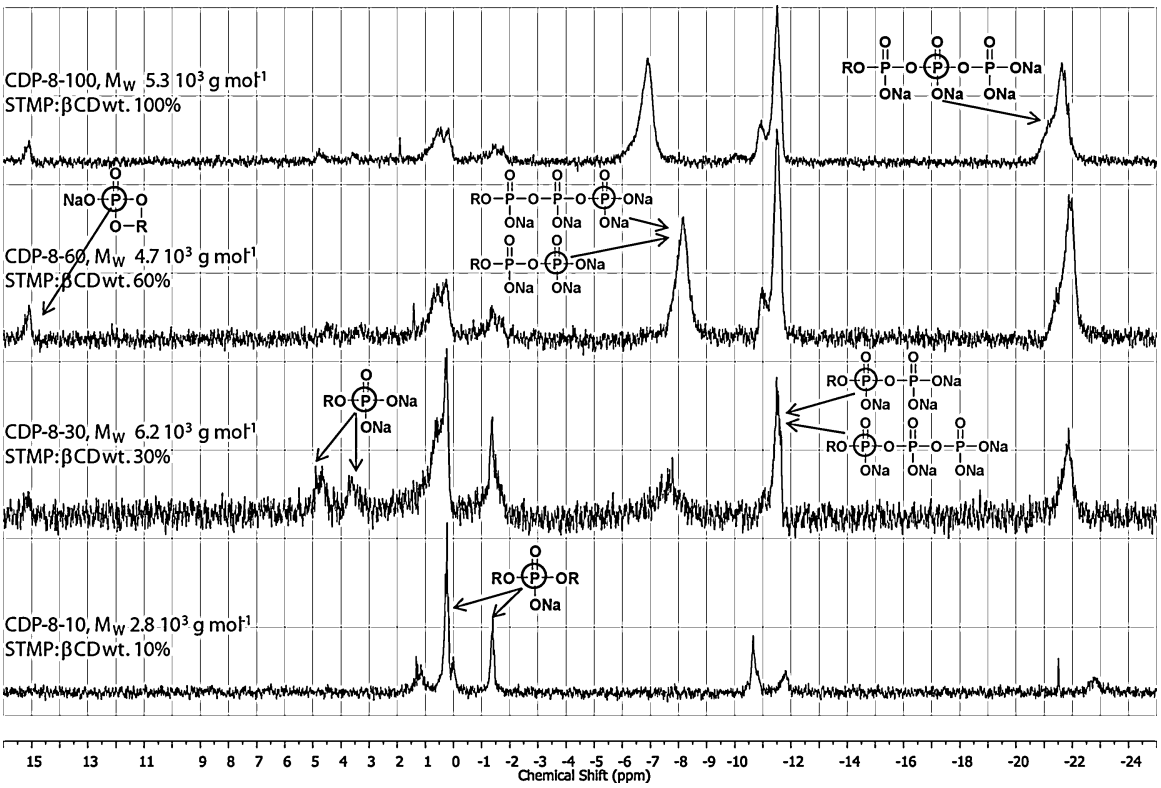

Fig. 3. ^{31}P NMR spectra in D_2O of CDPs synthesized at a NaOH:βCD weight ratio of 8% and with increasing STMP:βCD weight ratios.

The obtained polymers were also characterized by NMR in D_2O. The ^{1}H and ^{13}C spectra of CDP-20-60b are given in Figures S2 and S3 in comparison with those of βCD. A broadening of the different peaks is observed due to the combined effects of structural heterogeneities and dynamical constraints. Otherwise, the ^{31}P signals were assigned by comparison with chemical shifts reported in the literature (Lack et al., 2007; Sang et al., 2007). Examples of spectra are provided in Figs. 3 and 4. It must be noted that, as the solutions were extensively dialyzed, the final products should not contain inorganic phosphates such as STMP, STPP, PPi

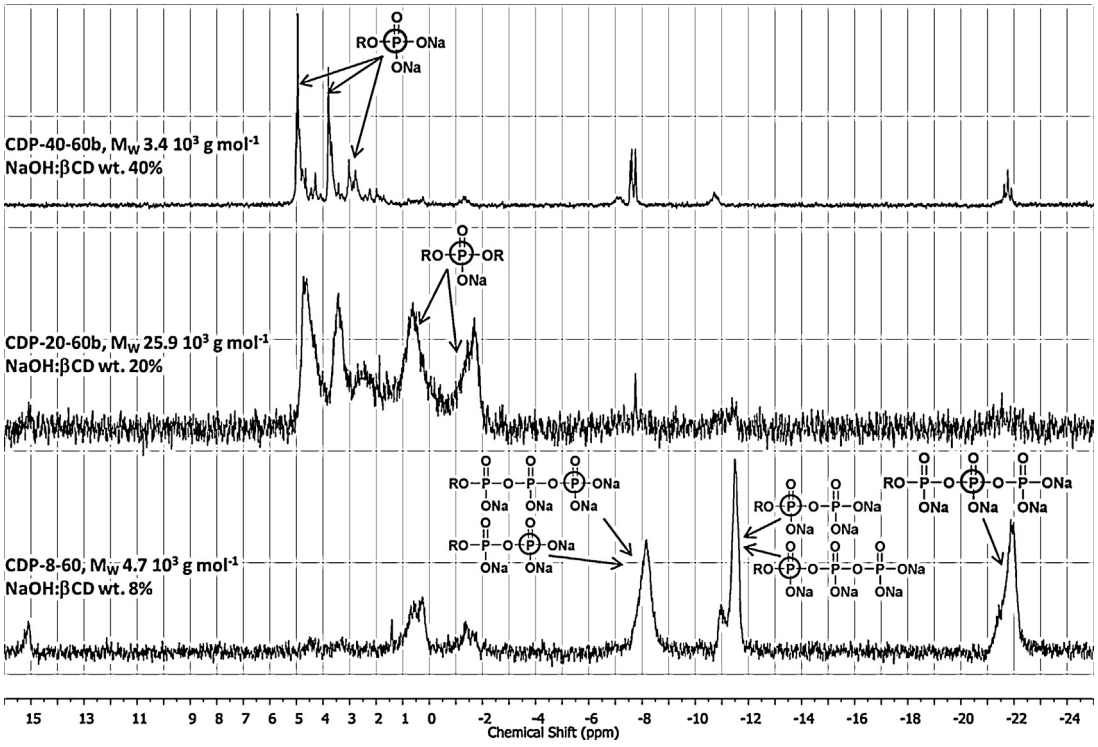

Fig. 4. ^{31}P NMR spectra in D_2O of CDPs synthesized at a STMP:βCD weight ratio of 60% and with increasing NaOH:βCD weight ratios.

and Pi. Fig. 3 includes the CDP spectra obtained at low NaOH:βCD weight ratio (8%), all the recovered polymers in this case having $M_w < 10^4$ g mol^{-1}. Analysis of the four spectra indicates that several features in the ^{31}P NMR spectra depend on the STMP:βCD weight ratio. At the lowest ratio (10%), monophosphate linkages between βCDs are predominant as indicated by the signals between δ −2 and 2 ppm (Pc signal). An increase in STMP:βCD weight ratio generates new peaks associated to grafted tripolyphosphates (TPPg) or pyrophosphates (PPg), and observed in three zones (δ −9 to −6 ppm, δ −12 to −10 ppm, δ −22 to −20 ppm). It had been shown that PPg is usually formed in negligible amounts at pH > 12, so the observed peaks should be mainly related to TPPg (Lack et al., 2007; Sang et al., 2007). Increasing STMP:βCD intensifies the signals for TPPg, up to the point they become predominant. In addition, the results indicate that, under the used conditions (NaOH:βCD of 8%), TPPg units are not significantly hydrolyzed into Pg. Fig. 4 depicts the spectra obtained for CDPs prepared at a STMP:βCD weight ratio of 60%. M_w and the ^{31}P NMR spectra largely depend on the NaOH:βCD weight ratio. At the lowest ratio (8%), M_w is lower than 10^4 g mol^{-1}, and peaks other than those associated to the phosphate connecting units (Pc) are mainly related to TPPg. At a ratio of 20%, M_w is now higher than 10^4 g mol^{-1}, and two main sets of signals can be observed at δ −2 to 2 ppm for Pc and δ 2–5 ppm for Pg. The signals are broad, as expected for a polymer. In contrast to the previous conditions (NaOH:βCD weight ratio of 8%, see Fig. 3), the higher NaOH:βCD weight ratio (20%) used in these experiments induces the hydrolysis of TPPg into Pg units, as evidenced by the absence of TPPg peaks. At the highest NaOH:βCD weight ratio (40%), the main peaks can be assigned to grafted monophosphates (Pg), yet the M_w is again lower than 10^4 g mol^{-1}. This last observation suggests that too strong basic conditions also favour the hydrolysis of the monophosphate groups that link the βCDs together, decreasing the molecular weight of the compounds.

In summary, experimental conditions have been identified, allowing polymers with $M_w > 10^4$ g mol^{-1} to be synthesized. Favourable experimental conditions require a NaOH:βCD weight ratio of 20% and STMP:βCD weight ratios ≥60%. It should be noticed that, when higher STMP:βCD weight ratios (100–200%) are used, pendent tripolyphosphates (TPPg) are also formed as the hydrolysis of the previously grafted TTPg units are not complete (Figure S4).

3.2. Complex formation

The βCD binding properties of some of the obtained CDPs were investigated by isothermal titration microcalorimetry (ITC) using 1-adamantyl acetic acid as a guest, at 25 °C in a phosphate buffer (0.01 mol L^{-1}, pH 7.0, NaCl 1.0 mol L^{-1}). Adamantyl derivatives are known to form inclusion complex with βCD, the excellent match in size and shape between the adamantyl group and the βCD cavity leading to high binding constants and large enthalpic variation (Rekharsky & Inoue, 1998). Four polymers with M_w differing by more than one order of magnitude were tested, the native βCD being used as a benchmark. The results are reported in Table 2.

The complex formation is exothermic in all cases, as expected (representative enthalpograms are depicted in Figure S5).

Fig. 5. Direct visual observation of $CaCl_2$/CDP-20-150a mixtures at pH 9 (Ca^{2+}:P = 2.8, CDP-20-150a at 50, 25, 16.6, 12.5 and 8.3 g L^{-1} for tube 1–5, respectively).

As expected as well, the formation of inclusion complexes is an enthalpy-driven process ($\Delta H < 0$), with an unfavourable entropic contribution ($T\Delta S > 0$). The binding constant K decreases by 2 orders of magnitude between βCD (in this work, $K \sim 114 \times 10^3$ L mol^{-1}, in the literature $K \sim 118 \times 10^3$ L mol^{-1} (Charlot, Auzély-Velty, & Rinaudo, 2003)) and CDP-20-150a ($M_w \sim 59.2 \times 10^3$ g mol^{-1} and $K \sim 1.3 \times 10^3$ L mol^{-1}). This large decrease mainly reflects a reduced accessibility to the βCD cavity. Indeed, βCD units in the polymers are linked together by phosphate bridges, and they also bear several phosphate groups absent in the original βCD. Such a loss in accessibility, inducing a K decrease, has already been reported for substituted βCD (Carrazana, Jover, Meijide, Soto, & Vázquez Tato, 2005), and also for copolymers of βCD/epichlorohydrin (Nielsen, Wintgens, Amiel, Wimmer, & Larsen, 2010). CDP-8-10 and CDP-8-100 mainly differ by their phosphorus weight percentage, with a higher number of phosphate groups per βCD for CDP-8-100. As a result, the βCDs cavity becomes less accessible leading to a lower K (23.5×10^3 L mol^{-1} and 5.3×10^3 L mol^{-1} for CDP-8-10 and CDP-8-100, respectively). Only a slight decrease could be noticed when transitioning from CDP-20-60a to CDP-20-150a (4.05×10^3 L mol^{-1} to 1.3×10^3 L mol^{-1}) even if the number of βCDs per chain is quite different in these two polymers (a rough estimate indicates the presence of ∼16 and ∼33 βCDs per chain, respectively). This slight decrease in binding could be related to the presence of polyphosphate groups in CDP-20-150a (see Figure S4) that might lower βCDs accessibility. The stoichiometry of the binding reaction deviates from 1, in agreement with a reduced accessibility to the βCD cavity.

The interaction of some of the obtained CDPs with a divalent cation such as Ca^{2+} was first investigated qualitatively. At pH ≥ 8, addition of a CDP-20-150a solution ($M_w \sim 59.2 \times 10^3$ g mol^{-1}) into a $CaCl_2$ solution led to immediate precipitation at Ca^{2+}:P ratios higher than 2.5 and at polymer concentrations higher than 9 g L^{-1} (Fig. 5). On the contrary, mixture of CDP-8-30 ($M_w \sim 6.2 \times 10^3$ g mol^{-1}) and $CaCl_2$ did not lead to precipitation, whatever the experimental conditions. At pH < 8 and/or at lower

Table 2
Thermodynamic parameters measured at 25 °C for the inclusion complex formation of βCD and several CDPs with 1-adamantane acetic acid.

Polymer	βCD[a]	CDP-8-10[b]	CDP-8-100[b]	CDP-20-60a[b]	CDP-20-150a[b]
M_w (g mol^{-1})	1135	3.1×10^3	5.3×10^3	8.6×10^3	59.2×10^3
P (wt.%)		2.3	6.3	3.8	5.6
n	1.1	1.1	1.6	1.8	2.5
10^{-3} K (L mol^{-1})	114	23.5	5.3	4.05	1.3
ΔH (kJ mol^{-1})	−23.47	−20.41	−17.90	−11.32	−11.60
$T\Delta S$ (kJ mol^{-1})	5.36	4.51	3.36	9.24	4.96

[a] In 0.15 mol L^{-1} NaCl.
[b] In 1.0 mol L^{-1} NaCl.

Table 3
Thermodynamic parameters measured at 25 °C for the interactions of several CDPs with Ca^{2+} cation.

Polymer	CDP-8-30	CDP-8-100	CDP-20-60c	CDP-20-150a	
M_w (g mol^{-1})	6.2×10^3	5.3×10^3	25.9×10^3	59.2×10^3	
P (wt.%)	3.3	6.3	4.8	5.6	
$n = [Ca^{2+}]/[P]$	0.16	0.15	0.44	0.50	0.65[a]
10^{-4} K (L mol^{-1})	1.04	0.97	3.84	4.34	4.25[a]
ΔH (kJ mol^{-1})	12.4	12.5	9.4	8.1	8.8[a]
$T\Delta S$ (kJ mol^{-1})	35.3	35.3	35.5	34.6	35.2[a]

[a] pH = 8.5.

polymer concentrations (<8 g L^{-1}), the different mixtures were always clear. ITC measurements were run to quantify the interactions of the CDPs with $CaCl_2$ (representative enthalpograms are available in Figure S6). The obtained results are reported in Table 3 for several CDPs characterized by M_w lower or higher than 10^4 g mol^{-1}, and different phosphorus content. The experiment with CDP-20-150a was run both at pH7 and pH8.5, the obtained results being quite comparable. The binding constants are relatively high, ~1 to 4×10^4 L mol^{-1}, the highest values being obtained for the CDPs with the highest M_w. As a comparison, it must be noted that lower values ranging from 1×10^3 L mol^{-1} (Canabady-Rochelle, Sanchez, Mellema, & Banon, 2009) to 4.9×10^3 L mol^{-1} (Zidane et al., 2012), have been determined for 1–25 β-caseino phosphopeptides by ITC. The affinity of other phosphate ligands for Ca^{2+} has also been measured by calcium ion-selective electrode (Mekmene & Gaucheron, 2011). For example for O-phospho-L-serine (only one phosphate group), a much lower binding constant (~10^3 L mol^{-1}) was obtained than the one measured for disodium hydrogen pyrophosphate (5.57×10^5 L mol^{-1}). The high affinity of pyrophosphate to Ca^{2+} makes it a calcium-chelating agent commonly used as melting salt in dairy products (Ozcan, Lucey, & Horne, 2008). The values we obtained for the studied phosphated CDPs are included in between those two values. CDP-8-30 and CDP-8-100 exhibit the same K values, of about 1×10^4 L mol^{-1}. These two polymers have about 3–4 βCDs by chain and phosphorus weight percentages differing by almost a factor of 2, suggesting more pyrophosphate and tripolyphosphate groups in CDP-8-100, in agreement with ^{31}P NMR spectra (Fig. 3). CDP-20-60a and CDP-20-150a feature higher K values, of about 4×10^4 L mol^{-1}. They have approximately 16 and 33 βCDs by chain, respectively, yet CDP-20-60c contains almost no pyrophosphate and tripolyphosphate groups as opposed to CDP-20-150a (^{31}P NMR spectra in Figure S2). Therefore, we suggest that the efficient Ca^{2+} chelation by CDPs is not related to the presence of pyrophosphate and tripolyphosphate groups, but is mainly due to the close proximity of monophosphate groups grafted on the βCD unit (and also to monophosphate units linking the βCDs). Based on this model, increasing the number of βCDs per chain will indeed strengthen chelation. The model is also in agreement with the observed n values. These are much lower for CDP-8-30 and CDP-8-100 (~0.15)

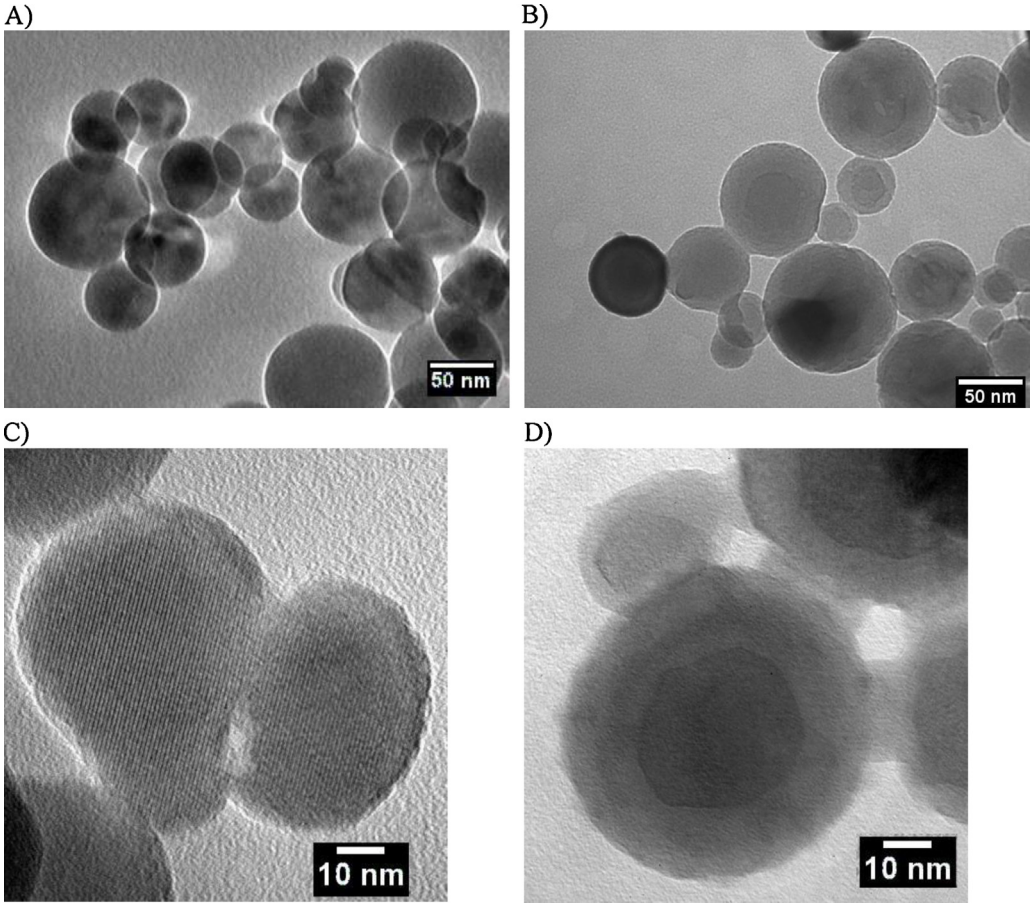

Fig. 6. Transmission electron micrographs of (A) HA dispersed in water and (B) HA dispersed in CDP-20-150a at 25 g L^{-1}.

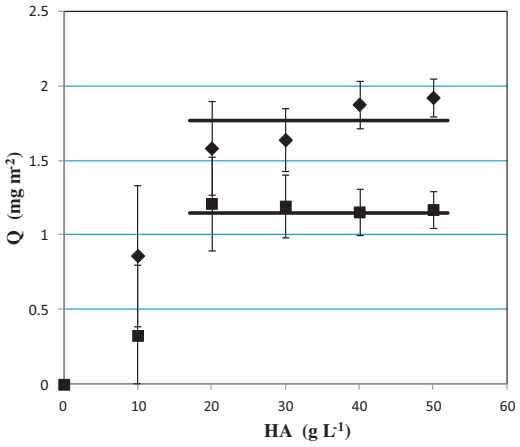

Fig. 7. Amounts of CDP adsorbed on HA particles as a function of HA concentration, for (■) CDP-8-30 and (♦) CDP-20-150a.

than for CDP-20-60c and CDP-20-150a (~0.47), implying that the CDPs with the higher M_w can chelate 3 times more Ca^{2+} ions (in molar ratios). As expected, the process is endothermic and largely entropically driven, with $\Delta H > 0$ and $T\Delta S \gg \Delta H$. This last feature could be explained by the release of water molecules from the hydrated phosphated polymers and/or from the hydrated Ca^{2+} ion, upon complex formation (Zidane et al., 2012).

3.3. Interactions with hydroxyapatite

The hydroxyapatite (HA) used in this work is a dry commercial HA nanopowder. At first, the HA samples (10 g L^{-1}) were dispersed in pure water or in CDP solution (CDP-8-30 or CDP-20-150a at 10 or 50 g L^{-1}), yet even after 180 min in an ultrasonic bath, HA was not well-dispersed in pure water as indicated by DLS measurements that showed very high polydispersity indices (PDI > 0.6). Interestingly, HA in a CDP solution was better dispersed, DLS measurements indicating a main diameter of about 250 nm (PDI ~ 0.3). The CDP covering the HA nanoparticles obviously favours a better dispersion in solution. It should be noticed that the same experiment conducted with a neutral epichlorohydrin/βCD copolymer ($M_w \sim 34.55 \times 10^3$ g mol^{-1}) did not provide a better HA dispersion than in water. In order to characterize the layer of CDP covering the HA nanoparticle surface, imaging and analytical experiments were performed. First, the HA nanoparticles were observed by transmission electron microscopy (TEM). Fig. 6 shows two micrographs of HA dispersed either in water or in a CDP-20-150a solution (in this latter case, the suspension was centrifuged and re-dispersed in water to eliminate the polymer excess). One can notice in Fig. 6A that the commercial HA nanoparticles are spherical and quite polydisperse, with diameters ranging from 50 to 150 nm; a few particles with very large diameters, i.e. over 700 nm, could also be detected on the grid (micrograph not shown). The detailed structure of HA particles is shown in Fig. 6C. One can see the crystalline structure of HA and the regular shape of the particles. Fig. 6B (observation performed at −170 °C in order to decrease CDP degradation induced by the electron beam) shows that most particles present a darker core with a lighter corona. This could agree with a core-corona structure, HA and CDP-20-150a being the core and corona, respectively. This CDP corona is unambiguously observed at higher magnification in Fig. 6D. We also quantified the amounts of CDP adsorbed on HA surface, *Q*. Varying amounts of HA were placed in the same volume of CDP (concentration fixed at 0.2 g L^{-1}). After 1 h in an ultrasonic bath and centrifugation, the supernatant concentration was determined by total carbon (TC) measurements. Fig. 7 reports the *Q* values as a function of HA concentration, and shows steep variations for each CDP. Except for the lowest HA concentration (1 g L^{-1}) where the errors on *Q* are too large to take the values into account, constant *Q* values were observed for the full HA concentration range. This behaviour reflects the strong affinity of CDP for the HA surfaces. Several phosphorus-containing compounds have been reported in the literature for their strong affinity towards HA surfaces, a feature attributed to chelation of the phosphonate functional groups with the calcium ions of the HA surfaces (Liu et al., 2007; Monge et al., 2011; Skartsila & Spanos, 2012). The same mechanism should occur in the case of CDPs in agreement with the good affinity between these polymers and Ca^{2+} as shown by the previous ITC experiments in solution (Table 3). Moreover, adsorption of neutral epichlorohydrin/βCD copolymer onto mineral or organic surfaces (Wintgens & Amiel, 2005; El Fagui et al., 2011) has shown milder adsorption isotherms, reflecting lower surface affinities than CDPs for HA surfaces. Finally, one can also notice that the plateau adsorbed amounts, 1.15 and 1.77 mg m^{-2} for CDP-8-30 and CDP-20-150a, respectively, correlate with the polymer molecular weight. A lower value of 0.5 mg m^{-2} had been reported for the adsorption of phospho-L-serine molecules onto HA microparticles (Skartsila & Spanos, 2012), these molecules adsorbing in the form of a monolayer. Grafting of hydroxyapatite/beta-tricalcium phosphate with βCD (achieved via a two-step reaction) leads to a βCD surface concentration of 1 mg m^{-2} (Jacobsen et al., 2012). In the case of polymers, the adsorbed amounts should depend strongly on their surface conformation. Polymers with a branched architecture, as is probably the case in the present study, cannot lie flat on the surface, and should prefer adsorbing when under coiled conformations. The increasing size of the polymer coils with the molecular weight (R_h ~3.4 and ~6.7 nm for CDP-8-30 and CDP-20-150a in NaCl 0.5 mol L^{-1}, respectively) might explain the trends observed in the present study.

4. Conclusion

This paper demonstrates that novel phosphorus containing cyclodextrin polymers (CDP) can be synthesized using "green chemistry" conditions as the reactions occur in aqueous media in presence of SMTP, a non-toxic reagent already used in the food industry. The reactions generally yield low molecular weight oligomers, except under optimized conditions (reactants and NaOH concentrations, temperature and reaction time) where polymers with molecular weight larger than 10^4 can be obtained. CDPs are hydrophilic polymers with anionic charges, and accordingly show large affinities for amphiphilic guests and calcium ions, as well as for hydroxyapatite surfaces. Composed mainly of β-cyclodextrin units and phosphated moieties, CDPs should be nontoxic, and combine the complexing abilities of its components. This makes CDP polymers very promising materials for numerous biomaterials applications, including as carriers for bioactive molecules or bone regeneration.

Acknowledgements

The authors are grateful to F. Caron and L. Najemi for their contribution to the polymer synthesis, and to D. Dragoe for the ICP analysis. The authors gratefully acknowledge financial support from CPER for the purchase of a TOC-L CSN from Shimadzu, and EU contribution through the NANOS3 project (Grant No. 290251) of the FP7-PEOPLE-2011-ITN call.

Appendix A. Supplementary data

Supplementary data associated with this article can be found, in the online version, at http://dx.doi.org/10.1016/j.carbpol.2013.06.073.

References

Abed, A., Assoul, N., Ba, M., Derkaoui, S. M., Portes, P., Louedec, L., et al. (2011). Influence of polysaccharide composition on the biocompatibility of pullulan/dextran-based hydrogels. *Journal of Biomedical Materials Research Part A*, *96A*, 535–542.

Ai, H., Xu, K., Liu, H., Chen, M., & Zhang, X. (2009). Synthesis, characterization, and curing properties of novel phosphorus-containing naphthyl epoxy systems. *Journal of Applied Polymer Science*, *113*, 541–546.

Akgun, B., Savci, E., & Avci, D. (2012). Synthesis and polymerizations of phosphonated-bis(methacrylamide)s for dental applications. *Journal of Polymer Science Part A: Polymer Chemistry*, *50*, 801–810.

Ansari, K. A., Vavia, P. R., Trotta, F., & Cavalli, R. (2011). Cyclodextrin-based nanosponges for delivery of resveratrol: In vitro characterisation, stability, cytotoxicity and permeation study. *AAPS PharmSciTech*, *12*, 279–286.

Autissier, A., Letourneur, D., & Le Visage, C. (2007). Pullulan-based hydrogel for smooth muscle cell culture. *Journal of Biomedical Materials Research Part A*, *82A*, 336–342.

Autissier, A., Visage, C. L., Pouzet, C., Chaubet, F., & Letourneur, D. (2010). Fabrication of porous polysaccharide-based scaffolds using a combined freeze-drying/cross-linking process. *Acta Biomaterialia*, *6*, 3640–3648.

Bejenariu, A., Popa, M., Dulong, V., Picton, L., & Le Cerf, D. (2009). Trisodium trimetaphosphate crosslinked xanthan networks: Synthesis, swelling, loading and releasing behaviour. *Polymer Bulletin*, *62*, 525–538.

Bilensoy, E. (2011). *Cyclodextrins in pharmaceutics, cosmetics, and biomedicine: Current and future industrial applications*. Hoboken, NJ: John Wiley & Sons, Inc.

Canabady-Rochelle, L.-S., Sanchez, C., Mellema, M., & Banon, S. (2009). Thermodynamic characterization of calcium–milk protein interaction by isothermal titration calorimetry. *Dairy Science and Technology*, *89*, 257–267.

Carrazana, J., Jover, A., Meijide, F., Soto, V. H., & Vázquez Tato, J. (2005). Complexation of adamantyl compounds by β-cyclodextrin and monoaminoderivatives. *The Journal of Physical Chemistry B*, *109*, 9719–9726.

Cesteros, L. C., Ramírez, C. A., Peciña, A., & Katime, I. (2007). Synthesis and properties of hydrophilic networks based on poly(ethylene glycol) and -cyclodextrin. *Macromolecular Chemistry and Physics*, *208*, 1764–1772.

Chaouat, M., Le Visage, C., Baille, W. E., Escoubet, B., Chaubet, F., Mateescu, M. A., et al. (2008). A novel cross-linked poly(vinyl alcohol) (PVA) for vascular grafts. *Advanced Functional Materials*, *18*, 2855–2861.

Charlot, A., Auzély-Velty, R., & Rinaudo, M. (2003). Specific interactions in model charged polysaccharide systems. *Journal of Physical Chemistry B*, *107*, 8248–8254.

Chaubal, M. V., Gupta, A. S., Lopina, S. T., & Bruley, D. F. (2003). Polyphosphates and other phosphorus-containing polymers for drug delivery applications. *Critical Reviews in Therapeutic Drug Carrier Systems*, *20*, 22.

El Fagui, A., Dalmas, F., Lorthioir, C., Wintgens, V., Volet, G., & Amiel, C. (2011). Well-defined core–shell nanoparticles containing cyclodextrin in the shell: A comprehensive study. *Polymer*, *52*, 3752–3761.

García-Zubiria, Í. X., González-Gaitanoa, G., & Isasi, J. R. (2007). Isosteric heats of sorption of 1-naphthol and phenol from aqueous solutions by β-cyclodextrin polymers. *Journal of Colloid and Interface Science*, *307*, 64–70.

Georgieva, R., Tsevi, R., Kossev, K., Kusheva, R., Balgjiska, M., Petrova, R., et al. (2002). Immobilization of aminothiols on poly(oxyalkylene phosphates). Formation of poly(oxyethylene phosphates)/cysteamine complexes and their radioprotective efficiency. *Journal of Medicinal Chemistry*, *45*, 5797–5801.

Grachek, V. I., Shunkevich, A. A., & Martsynkevich, R. V. (2011). Synthesis and sorption properties of new fibrous nitrogen- and phosphorus-containing ion exchangers. *Russian Journal of Applied Chemistry*, *84*, 1335–1340.

Huang, S.-W., & Zhuo, R.-X. (2008). Recent advances in polyphosphoester and polyphosphoramidate-based biomaterials. *Phosphorus, Sulfur, and Silicon and the Related Elements*, *183*, 340–348.

Inoue, H., Nakayama, H., & Tsuhako, M. (2000). A one-step phosphorylation of d-aldohexoses and d-aldopentoses with inorganic cyclo-triphosphate. *Carbohydrate Research*, *324*, 10–16.

Inoue, H., Tone, N., Nakayama, H., & Tsuhako, M. (2003). Stereoselective phosphorylation of branched cyclodextrins with inorganic cyclo-triphosphate. *Carbohydrate Research*, *338*, 2067–2074.

Jacobsen, P., Nielsen, J., Juhl, M., Theilgaard, N., & Larsen, K. (2012). Grafting cyclodextrins to calcium phosphate ceramics for biomedical applications. *Journal of Inclusion Phenomena and Macrocyclic Chemistry*, *72*, 173–181.

Khan, A. R., Forgo, P., Stine, K. J., & D'Souza, V. T. (1998). Methods for selective modifications of cyclodextrins. *Chemical Reviews*, *98*, 1977–1996.

Khondkar, D., Tester, R. F., Hudson, N., Karkalas, J., & Morrow, J. (2007). Rheological behaviour of uncross-linked and cross-linked gelatinised waxy maize starch with pectin gels. *Food Hydrocolloids*, *21*, 1296–1301.

Lack, S., Dulong, V., Le Cerf, D., Picton, L., Argillier, J. F., & Muller, G. (2004). Hydrogels Based on Pullulan Crosslinked with sodium trimetaphosphate (STMP): Rheological study. *Polymer Bulletin*, *52*, 429–436.

Lack, S., Dulong, V., Picton, L., Cerf, D. L., & Condamine, E. (2007). High-resolution nuclear magnetic resonance spectroscopy studies of polysaccharides crosslinked by sodium trimetaphosphate: A proposal for the reaction mechanism. *Carbohydrate Research*, *342*, 943–953.

Lakshmi, M. S., Ashwaq, H. H. O., & Reddy, B. S. R. (2011). Synthesis and characterization of novel phosphorous-coupling agent for use as compatibilizer, flame retardant, hardener and adhesion promoter in making polymer networks. *Polymer-Plastics Technology and Engineering*, *50*, 266–275.

Layre, A.-M., Wintgens, V., Gosselet, N.-M., Dalmas, F., & Amiel, C. (2009). Tuning the interactions in cyclodextrin polymer nanoassemblies. *European Polymer Journal*, *45*, 3016–3026.

Le Bail, P., Morin, F. G., & Marchessault, R. H. (1999). Characterization of a crosslinked high amylose starch excipient. *International Journal of Biological Macromolecules*, *26*, 193–200.

Leprêtre, S., Chai, F., Hornez, J.-C., Vermet, G., Neut, C., Descamps, M., et al. (2009). Prolonged local antibiotics delivery from hydroxyapatite functionalised with cyclodextrin polymers. *Biomaterials*, *30*, 6086–6093.

Li, B.-Z., Wang, L.-j., Li, D., Chiu, Y. L., Zhang, Z.-j., Shi, J., et al. (2009). Physical properties and loading capacity of starch-based microparticles crosslinked with trisodium trimetaphosphate. *Journal of Food Engineering*, *92*, 255–260.

Li, S., & Purdy, W. C. (1992). Cyclodextrins and their applications in analytical chemistry. *Chemical Reviews*, *92*, 1457–1470.

Liu, X.-M., Lee, H.-T., Reinhardt, R. A., Marky, L. A., & Wang, D. (2007). Novel biomineral-binding cyclodextrins for controlled drug delivery in the oral cavity. *Journal of Controlled Release*, *122*, 54–62.

Liu, X.-M., Wiswall, A. T., Rutledge, J. E., Akhter, M. P., Cullen, D. M., Reinhardt, R. A., et al. (2008). Osteotropic β-cyclodextrin for local bone regeneration. *Biomaterials*, *29*, 1686–1692.

Loftsson, T., & Duchêne, D. (2007). Cyclodextrins and their pharmaceutical applications. *International Journal of Pharmaceutics*, *329*, 1–11.

Mekmene, O., & Gaucheron, F. (2011). Determination of calcium-binding constants of caseins, phosphoserine, citrate and pyrophosphate: A modelling approach using free calcium measurement. *Food Chemistry*, *127*, 676–682.

Mocanu, G., Mihai, D., Picton, L., LeCerf, D., & Muller, G. (2002). Associative pullulan gels and their interaction with biological active substances. *Journal of Controlled Release*, *83*, 41–51.

Monge, S., Canniccioni, B., Graillot, A., & Robin, J.-J. (2011). Phosphorus-containing polymers: A great opportunity for the biomedical field. *Biomacromolecules*, *12*, 1973–1982.

Mou, L., Singh, G., & Nicholson, J. W. (2000). Synthesis of a hydrophilic phosphonic acid monomer for dental materials. *Chemical Communications*, 345–346.

Nielsen, T. T., Wintgens, V., Amiel, C., Wimmer, R., & Larsen, K. L. (2010). Facile synthesis of β-cyclodextrin-dextran polymers by "click" chemistry. *Biomacromolecules*, *11*, 1710–1715.

Ozcan, T., Lucey, J. A., & Horne, D. S. (2008). Effect of tetrasodium pyrophosphate on the physicochemical properties of yogurt gels. *Journal of Dairy Science*, *91*, 4492–4500.

Pariot, N., Edwards-Lévy, F., Andry, M.-C., & Lévy, M.-C. (2000). Cross-linked β-cyclodextrin microcapsules: Preparation and properties. *International Journal of Pharmaceutics*, *211*, 19–27.

Pasqui, D., Rossi, A., Di Cintio, F., & Barbucci, R. (2007). Functionalized titanium oxide surfaces with phosphated carboxymethyl cellulose: Characterization and bonelike cell behavior. *Biomacromolecules*, *8*, 3965–3972.

Rekharsky, M. V., & Inoue, Y. (1998). Complexation thermodynamics of cyclodextrins. *Chemical Reviews*, *98*, 1875–1917.

Renard, E., Deratani, A., Volet, G., & Sébille, B. (1997). Preparation and characterization of water soluble high molecular weigth β-cyclodextrin-epichlorhydrin polymers. *European Polymer Journal*, *33*, 49–53.

San Juan, A. l., Bala, M., Hlawaty, H., Portes, P., Vranckx, R., Feldman, L. J., et al. (2009). Development of a functionalized polymer for stent coating in the arterial delivery of small interfering RNA. *Biomacromolecules*, *10*, 3074–3080.

Sang, Y., Prakash, O., & Seib, P. A. (2007). Characterization of phosphorylated cross-linked resistant starch by 31P nuclear magnetic resonance (^{31}P NMR) spectroscopy. *Carbohydrate Polymers*, *67*, 201–212.

Sang, Y., Seib, P. A., Herrera, A. I., Prakash, O., & Shi, Y.-C. (2010). Effects of alkaline treatment on the structure of phosphorylated wheat starch and its digestibility. *Food Chemistry*, *118*, 323–327.

Skartsila, K., & Spanos, N. (2012). Adsorption monitoring of phospho-L-serine on hydroxyapatite. *Colloid and Polymer Science*, *290*, 731–739.

Suzuki, S., Whittaker, M. R., Grøndahl, L., Monteiro, M. J., & Wentrup-Byrne, E. (2006). Synthesis of soluble phosphate polymers by RAFT and their in vitro mineralization. *Biomacromolecules*, *7*, 3178–3187.

Szejtli, J. (2004). Past, present and future of cyclodextrin research. *Pure and Applied Chemistry*, *76*, 1825–1845.

Tarelli, E., Lemercinier, X., & Wheeler, S. (1997). Direct preparation of cyclodextrin monophosphates. *Carbohydrate Research*, *302*, 27–34.

Uekama, K. (2004). Design and evaluation of cyclodextrin-based drug delivery. *Chemical and Pharmaceutical Bulletin*, *52*, 900–915.

Wintgens, V., & Amiel, C. (2005). Surface plasmon resonance study of the interaction of β-cyclodextrin polymer and hydrophobically modified poly-(*N*-isopropylacrylamide). *Langmuir*, *21*, 11455–11461.

Woo, K., & Seib, P. A. (1997). Cross-linking of wheat starch and hydroxypropylated wheat starch in alkaline slurry with sodium trimetaphosphate. *Carbohydrate Polymer*, *33*, 263–271.

Xia, X.-N., Lu, Y.-B., Zhou, X., Xiong, Y.-Q., Zhang, X.-H., & Xu, W.-J. (2006). Synthesis of novel phosphorous-containing biphenol, 2-(5,5-dimethyl-4-phenyl-2-oxy-1,3,2-dioxaphosphorin-6-yl)-1,4-benzenediol and its application as flame-retardant in epoxy resin. *Journal of Applied Polymer Science*, *102*, 3842–3847.

Zidane, F., Matéos, A., Cakir-Kiefer, C., Miclo, L., Rahuel-Clermont, S., Girardet, J.-M., et al. (2012). Binding of divalent metal ions to 1–25 β-caseinophosphopeptide: An isothermal titration calorimetry study. *Food Chemistry*, *132*, 391–398.